Cardiovascular Research (2011) **89**, 816–824
doi:10.1093/cvr/cvq336

Time course and mechanisms of endo-epicardial electrical dissociation during atrial fibrillation in the goat

Jens Eckstein[1,2]*, Bart Maesen[1], Dominik Linz[1], Stef Zeemering[1], Arne van Hunnik[1], Sander Verheule[1], Maurits Allessie[1], and Ulrich Schotten[1]

[1]Department of Physiology, Maastricht University, Maastricht, The Netherlands; and [2]Department of Medicine, University Hospital Basel, Petersgraben 4, CH 4031 Basel, Switzerland

Received 5 July 2010; revised 30 September 2010; accepted 21 October 2010; online publish-ahead-of-print 26 October 2010

Time for primary review: 30 days

Aims This study aims to determine the degree and mechanisms of endo-epicardial dissociation of electrical activity during atrial fibrillation (AF) and endo-epicardial differences in atrial electrophysiology at different stages of atrial remodelling.

Methods and results Simultaneous high-density endo-epicardial mapping of AF was performed on left atrial free walls of goats with acute AF, after 3 weeks, and after 6 months of AF (all $n = 7$). Endo-epicardial activation time differences and differences in the direction of conduction vectors were calculated, endocardial and epicardial effective refractory periods (ERP) were determined, and fractionation of electrograms was quantified. Histograms of endo-epicardial activation time differences and differences in the direction of conduction vectors revealed two distinct populations, i.e. dissociated and non-dissociated activity. Dyssynchronous activity (dissociated in time) increased from 17 ± 7% during acute AF to 39 ± 17% after 3 weeks, and 68 ± 13% after 6 months of AF. Dissociation was more pronounced in thicker parts of the atrial wall (thick: 49.3 ± 21.4%, thin: 42.2 ± 19.0%, $P < 0.05$). At baseline, endocardial ERPs were longer when compared with epicardial ERPs (ΔERP, 21.8 ± 18 ms; $P < 0.001$). This difference was absent after 6 months of AF. The percentage of fractionated electrograms during rapid pacing increased from 9.4 ± 1.9% (baseline) to 18.6 ± 0.6% (6 months).

Conclusion During AF, pronounced dissociation of electrical activity occurs between the epicardial layer and the endocardial bundle network. The increase in dissociation is due to owing to progressive uncoupling between the epicardial layer and the endocardial bundles and correlates with increasing stability and complexity of the AF substrate.

Keywords Atrial fibrillation • Conduction • Endo-epicardial mapping • Dissociation • Remodelling

1. Introduction

Atrial fibrillation (AF) is a progressive arrhythmia.[1] Mechanisms underlying the increasing duration of AF episodes and the loss of efficacy of current therapeutic interventions over time have been subject of extensive research.[2–4] Shortening of refractoriness and wavelength certainly contributes to, but cannot fully explain, increased AF stability.[4,5] Disruption of electrical side-to-side connections between muscle bundles resulting in longitudinal dissociation of electrical activity has been identified as a key element in the development of a substrate of AF.[6–8] Whether such dissociation of electrical activity also occurs between the epicardial layer and the endocardial bundle network and how this endo-epicardial electrical dissociation (EED) develops during atrial remodelling is currently unknown. EED might enlarge the functional surface area available for wavefront propagation and has been proposed as prerequisite condition for transmural conduction and 'breakthrough'.[9] Despite its potential role of EED for AF stability, only very few studies investigated simultaneous endo-epicardial activation patterns during AF.[10,11] No data are currently available on the time course and the mechanisms of EED owing to progressive electrical and structural remodelling of the atria.

Our aim was to examine EED as a potential mechanism leading to increasing AF stability over time. We developed techniques for quantification of EED during AF, tested the hypothesis that the

*Corresponding author. Tel: +41 31 2652525; fax: +41 31 2654598, Email: ecksteinj@uhbs.ch

increasing stability of AF correlates with the electrical dissociation between the epicardial layer and the endocardial bundle network, and investigated the mechanisms underlying EED.

2. Methods

2.1 Model

In this study, the goat model of persistent AF was used.[5,8,12–14] Three groups of goats were included ($n = 7$ in each group). The group of sham-operated animals (acute AF as aAF) received a right atrial endocardial pacemaker lead (Medtronic Capsurefix®) 4 weeks prior to the open chest mapping study. In the 3 weeks AF group (3wAF), the lead was connected to a neurostimulator (Medtronic, Itrel1®). In the 6 months AF group (6mAF), an additional right atrial endocardial lead connected to a pacemaker (Medtronic Kappa®) was implanted to obtain atrial electrograms during *in vivo* cardioversion experiments. All animal procedures conformed to the US National Institutes of Health guidelines and were approved by the local ethical committee for animal experiments of Maastricht University.

2.2 Study protocol

2.2.1 Maintenance of AF

After 2 weeks of recovery from pacemaker implantation, AF was artificially maintained by repetitive 50 Hz burst pacing at three times threshold every other second. 3wAF goats were paced for 3 weeks. In the 6mAF group, pacing was performed every other second for the first 14 weeks followed by 1 s/min for the remaining 10 weeks. No pacing was performed in the aAF group.

2.2.2 Cardioversion experiments

To document increasing AF stability, all 6mAF goats underwent pharmacological cardioversion experiments with flecainide (0.1 mg/kg/min, i.v.). Endpoints were restoration of sinus rhythm (SR), ventricular arrhythmias, QRS prolongation of >100%, and 90 min infusion time. Fibrillation pacemakers were switched off at least 1 h prior to the cardioversion experiments to assess the incidence of spontaneous cardioversion.

2.2.3 Open chest experiments

Animals were anaesthetized with sufentanyl (6 μg/kg/h), midazolam (0.8 mg/kg/h), and pancuronium (0.3 mg/kg/h). After left-sided thoracotomy, a high-density endo-epicardial mapping device was positioned in the left atrium. The device was carefully closed to make contact with the endocardial bundle network and the epicardial surface. When satisfactory signals were present (sharp deflections in the absence of injury currents), the distance between the endocardial and the epicardial part of the device was fixed with a fixation screw (see Supplementary material online, *Figure S1*). A silver plate in the thoracic cavity served as indifferent electrode. Unipolar signals were recorded during AF and during atrial pacing using a custom-made 256-channel mapping amplifier (filtering bandwidth 0.1–400 Hz, sampling rate 1 kHz, A/D resolution 16 bits). In 16/21 experiments, the mapped area was marked at the end of the experiment and photographed from the endocardial side to correlate the endocardial bundle structure with the functional data recorded.

2.3 Histology

After rapid excision, the LA was separated from the heart and parts of the LA were fixed in buffered 4% formaldehyde and embedded in paraffin for histological evaluation. For this, tissue sections of 5 μm were fixed at 56°C overnight, deparaffinized, and rehydrated. Fibrosis was quantified on one to two sections per atrium (four to six fields per section). To determine cardiomyocyte diameters and distances between the myocytes (intermyocyte distance), LA sections were stained with haematoxylin & eosin. The mean cell diameter of 30–35 transversely cut cells and respective 40–50 shortest intermyocyte distance in all four directions within one bundle were used for analysis in each goat as described earlier.[8]

2.4 Analysis of fibrillation electrograms

Electrogram files recorded during AF (4s) were analysed using custom-made analysis software. Local activation times were identified by maximum negative dV/dt in each unipolar electrogram. Fibrillation maps were automatically constructed and independently edited by two researchers. Median AF cycle length (AFCL) was calculated using all fibrillation intervals of all electrodes. Conduction times were assessed by calculating the difference in activation time between each electrode and its neighbours. Conduction block was defined as conduction time between adjacent electrodes >8 ms (>12 ms for oblique electrode pairs), corresponding to a conduction velocity of <20 cm/s, which is comparable to the definition of conduction block commonly used.[15,16] Apparent conduction velocity was determined by plane fitting through each activation time point and all neighbouring activation times occurring within a time window of 8 ms (>12 ms for oblique electrode pairs, maximum square of 3 × 3 electrodes). The resulting plane then indicated local direction (orientation of the plane) and velocity (reciprocal value of the steepness of the plane) for each local activation point.

EED was quantified using three different methods:

(1) To obtain a simple measure of endo-epicardial dyssynchrony, endo-epicardial activation time difference at each of the 90 pairs of opposing electrodes was calculated. The percentage of all endo-epicardial activation time differences above a threshold time difference was defined as 'dyssynchronous' and plotted as a function of this threshold time difference. This method allowed for quantification of endo-epicardial dyssynchrony independent from assumptions of cut-off values for endo-epicardial conduction velocities.

(2) To account for dissociation owing to differences in either activation time or direction of propagation, EED was calculated from histograms of endo-epicardial differences in activation time or direction of local conduction vectors. Two distinct populations of differences in activation times or direction of local conduction vectors representing dissociated and non-dissociated activity were identified by fitting a two-component Gaussian function (for activation time differences), or a Gaussian/uniform mixture distribution (for differences in direction) to the histograms. The percentage of the area under the curve formed by the dissociated component was referred to as 'dissociation index' (see *Figure 1* for details).

(3) For quantification of spatial distribution of dissociation, the analysis of activation time histograms or conduction direction difference histograms could not be used because of the limited number of data pairs at each individual electrode (between 30 and 50). Instead, all data were analysed using dissociation thresholds derived from the activation time difference and direction difference histograms. Two times the standard deviation of the non-dissociated components was taken as individual dissociation threshold, implying that ~95% of the non-dissociated activity met this criterion. Activity was considered dissociated if either the activation time difference or the conduction direction difference criterion revealed dissociation for all nine closest opposing electrodes. For each electrode, the percentage of dissociation during an episode of 4 s was calculated and colour-coded. The resulting dissociation maps were then analysed for their local entropy to determine the degree of randomness of the distribution of dissociated and non-dissociated areas.[17] To test for a correlation between EED and the endocardial bundle network anatomy, bundle structures were marked manually and dissociation was calculated separately for the areas containing endocardial bundles (thick regions) and the spaces between the bundles (thin regions).

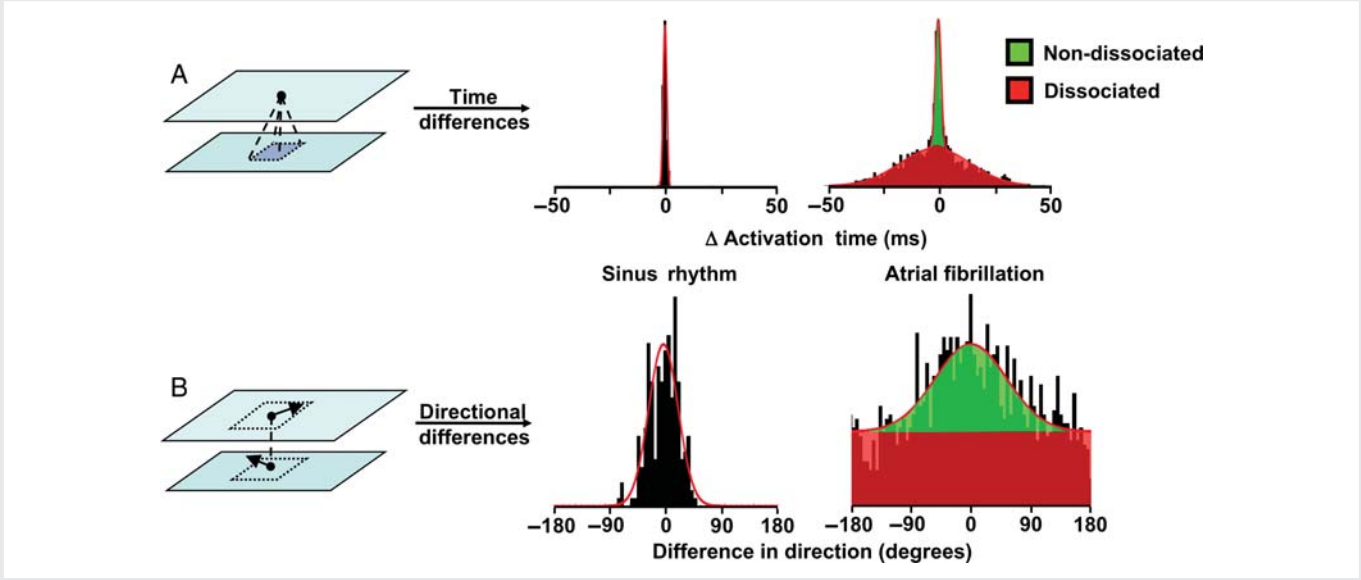

Figure 1 Curve-fitting method to quantify EED. (*A*) Calculation of the shortest endo-epicardial activation time difference for each electrode pair. To reduce the effect of spatial noise, the shortest activation time difference (normalized to the electrode distance) of the nine closest opposing electrodes was used for analysis (framed blue area on lower plane of the cartoon on the left). In the resulting histograms, the *x*-axes depict activation time differences (milliseconds) and the *y*-axes depict the number of events. While the histogram of activation time differences during SR can be fitted with a single-component Gaussian function, the histograms of activation time differences during AF are best-fitted with a two-component Gaussian mixture distribution.[26] This identifies two distinct populations representing non-dissociated activations (narrow component, small standard deviation, green) and dissociated activations (broad component, large standard deviation, red). (*B*) Calculation of the direction difference of corresponding local endocardial and epicardial conduction vectors (calculated based on the activation times of all neighbouring electrodes as dotted lines). Differences in direction can be fitted with a single-component Gaussian distribution during SR and a Gaussian/uniform mixture distribution with the Gaussian component representing concordant endo-epicardial activations (green) and the uniform component representing discordant endo-epicardial activation (red) during AF.

To quantify the occurrence of breakthrough, all activation times surrounded exclusively by identical or later activations—thus, representing starting points of waves in the mapping area—were identified and classified as peripheral wave (if located at the border of the mapping area) or breakthrough (if located within the mapping area). The incidence of breakthrough was then calculated as the number of wave starting points located within the mapping area per second.

2.5 Endo-epicardial dispersion of refractoriness and electrogram fractionation

To test the hypothesis that EED is because of endo-epicardial dispersion of refractoriness or electrical uncoupling between the epicardial layer and the endocardial bundle network, the animals were cardioverted to SR by internal DC shock with two 6 F defibrillation catheters (Elecath, Rahway, NJ, USA) positioned in the coronary sinus and in the posterior right atrium. Defibrillation was attempted with monophasic (5 ms) 5 J shock (Lifepak 9B, Medtronic Physio-Control Corp., Redmond, WA, USA). Energy was increased in steps of 5 J (maximum 20 J) until cardioversion was successful. ERP as well as electrogram fractionation were measured during atrial pacing. Local pacing threshold was determined separately for the endocardial and the epicardial pacing site and bipolar pacing (1.6 mm interelectrode distance) was performed from the centres of the electrode arrays at 250 and 400 ms basic cycle length (CL) at four times (current)-threshold. Only sites at which both the endocardial and epicardial threshold was low (<2 mA) were used for analysis. The longest S1–S2 interval (2 ms incremental steps) not resulting in a propagated response was taken as local ERP. Epicardial electrogram fractionation was determined during rapid pacing (CL = 200 ms) from a pacing site outside the mapping array. Atrial complexes showing two separate deflections, with a minimum amplitude of 25% of the larger deflection occurring within a time window of 2–15 ms were taken as 'short double potentials'.[18] 'Complex fractionated potentials' were defined as atrial complexes with three or more negative deflections.

2.6 Statistical analysis

All data are expressed as mean ± SD. Significance of differences in means between aAF, 3wAF, and 6mAF groups was calculated using a one-way analysis of variance with Newman–Keul's post-test and a paired Student's *t*-test for significance of differences in means between the endocardial and the epicardial layer in the same specimen. *P* values <0.05 were considered significant.

3. Results

3.1 Cardioversion experiments

The cardioversion experiments in the 6mAF group documented increasing AF stability over time. AF was persistent in all seven goats undergoing cardioversion experiments after 2 weeks of AF. At that time point, pharmacological cardioversion to SR was successful in 6 out of 7 goats (85%). The success rate declined to 3/7 (43%) after 6 weeks, 1/7 (14%) after 10 weeks, and 0/7 (0%) after 14 weeks. No animal that cardioverted successfully had failed to cardiovert at an earlier time point. Baseline AFCL did not differ significantly between 2 and 14 weeks of AF (116 ± 24 ms vs. 117 ± 21 ms, ns).

3.2 Enhanced heterogeneity of conduction in both the epicardial layer and the endocardial bundle network

Table 1 summarizes the basic electrophysiological parameters of AF found in the three groups of animals. During open chest experiments, the mean AFCL was significantly longer in the aAF group when compared with the 3wAF group ($P < 0.01$). No further shortening of the AFCL was found in the 6mAF group. The median (P_{50}) of normalized phase differences (in milliseconds/millimetre) as well as the heterogeneity index ($P_{95} - P_5)/P_{50}$) were significantly larger in the 6mAF and the 3wAF group when compared with the aAF group ($P < 0.05$). Incidence of conduction block between neighbouring electrodes was highest in the 6mAF and lowest in the aAF group ($P < 0.05$). There was a trend towards more conduction disturbances endocardially, but no significant differences in AFCL, heterogeneity indices, or incidence of conduction block between the epicardial layer and the endocardial bundle network.

Table 1 Basic electrophysiological parameters

	Acute	3 weeks	6 months
AFCL (ms)	141 ± 15	121 ± 10[a]	120 ± 5[a]
P_{50} phase differences (ms/mm)	0.7 ± 0.3	1.0 ± 0.4[a]	1.4 ± 0.2[a,b]
$P_{95} - P_5/P_{50}$ phase differences			
Endocardial	9.9 ± 3.4	14.6 ± 4.7[a]	13.0 ± 1.5[a]
Epicardial	7.4 ± 2.4	10.7 ± 3.2[a]	11.2 ± 1.8[a]
Incidence of block (% of activations)			
Endocardial	8.0 ± 3.8	15.7 ± 3.0[a]	17.4 ± 4.7[a,b]
Epicardial	6.0 ± 2.8	11.3 ± 4.9[a]	16.4 ± 2.9[a,b]

Significant electrical remodelling reflected by AFCL decrease (aAF vs. 3 weeks-AF), increasing conduction times, heterogeneity index ($P_{95} - P_5/P_{50}$ of conduction times), and increased incidence of block.
[a]Significant vs. aAF.
[b]Significant vs. 3 weeks-AF.

3.3 Endo-epicardial dissociation during AF

Figure 2 illustrates EED in a goat after 3 weeks of AF. For all goats, each of the three different quantification methods of EED showed an increase of dissociation with AF duration.

3.3.1 Dyssynchony of endo-epicardial activation

For any threshold of endo-epicardial activation time differences above 0 ms, the percentage of 'dyssynchronous' activation time differences was highest in the 6mAF group and lowest in the aAF group (*Figure 3*). Differences in dyssynchrony between groups were most pronounced at a threshold activation time difference of 10 ms. At this threshold value, the percentage of dyssynchronous activity was

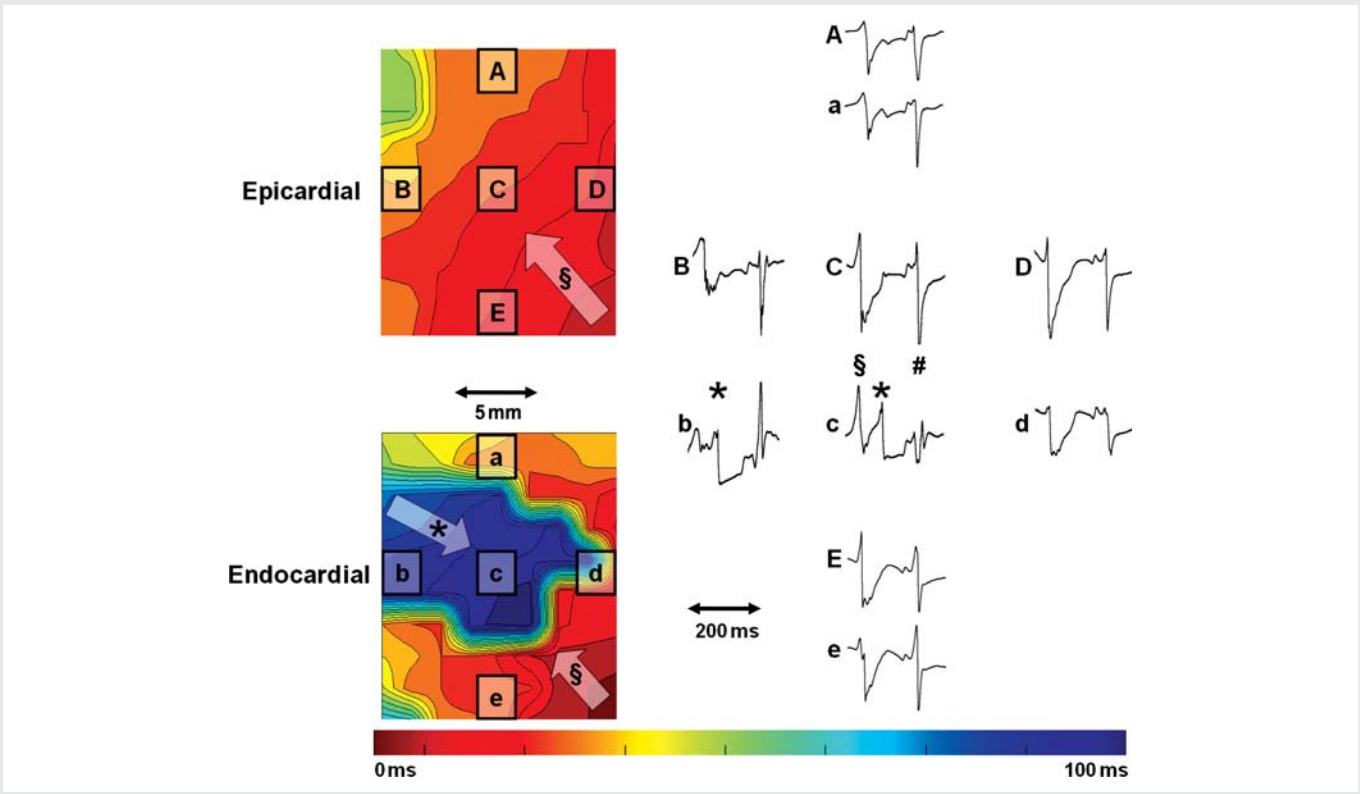

Figure 2 Endo-epicardial isochronal map (3wAF) of two exactly corresponding areas of the epicardial and endocardial layer. Time between isochrones 5 ms, early activations colour-coded in red, late in blue. Five corresponding electrogram tracings (epicardial A–E; endocardial a–e) are displayed on the right. A broad fibrillation wave enters the mapping area from the lower right corner, where it activates both the epicardial as well as the endocardial layer. The electrograms b and c show two deflections between 50 and 100 ms (marked by '§' and '*'). The deflections marked with '*' represent a wave that enters the mapping area from the left and which exclusively propagates within the endocardial layer (blue wave in isochronal map). The final deflections in the electrogram tracings represent the next wave, which again activates both layers of the atrial wall (not displayed in the isochronal map, electrograms marked with #).

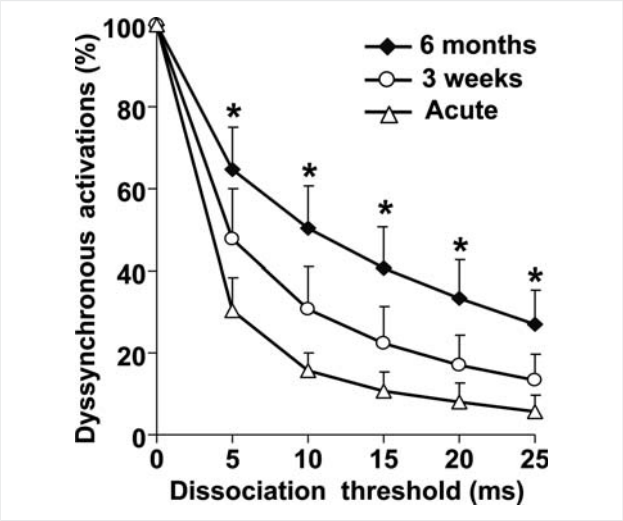

Figure 3 Percentage dyssynchronous activity as a function of the endo-epicardial activation time difference threshold. Y-axis: Percentage of activation time differences above various threshold activation time differences. X-axis: Activation time difference thresholds in milliseconds. *$P < 0.01$ vs. 3wAF and aAF.

50.3 ± 10.4% in the 6mAF group, 30.8 ± 10.3% in the 3wAF group, and 15.7 ± 4.4% in the aAF group ($P < 0.01$).

3.3.2 Histograms of endo-epicardial differences in activation time and direction of local conduction vectors

The histograms of activation time differences and differences in the direction of conduction vectors showed two distinct components with different behaviour. Calculations of histograms after artificial shift of endocardial against epicardial activation times suggest that the narrow component reflects a temporal or directional relation between electrical activity in the epicardial layer and the endocardial bundle network (i.e. non-dissociated electrical activity). The wide or uniform components reflect lack of such an inter-relation suggesting that epicardial layer and endocardial bundle network are activated independently (see Supplementary material online for further details).

Figure 4 shows histograms of activation time differences (panel A) and histograms of differences in the direction of propagation (panel B) for all 21 goats. During acute AF, the index of EED was 17 ± 7% based on the activation time difference criterion and 17 ± 10% based on the direction difference criterion. In the 3wAF group, the dissociation index increased significantly to 39 ± 17% (time criterion) and 53 ± 18% (direction criterion) ($P < 0.05$ compared with aAF). After 6 months of AF, as much as 68 ± 13% (time criterion) and 72 ± 14% (direction criterion) of the electrical activity was dissociated between the epicardial layer and the endocardial bundle network ($P < 0.05$ compared with aAF and 3wAF).

Interestingly, mean endo-epicardial activation time difference was close to 0 ms and not different in all three groups (aAF: 0.87 ± 3.04 ms, 3wAF: −0.82 ± 4.71 ms, 6mAF: −0.14 ± 1.23 ms, ns), arguing against preferential conduction from the epicardial layer to the endocardial bundles network or vice versa.

3.3.3 Spatial distribution of dissociation

Spatial analysis revealed that the degree of dissociation was not uniformly distributed over the mapping area but that there were areas with higher and lower degrees of EED (*Figure 5*, upper and left lower panel). To test for randomness, we calculated the entropy value for spatial distribution of dissociation (1 = random distribution, 0 = no randomness). There was no difference in entropy between groups (aAF: 0.63 ± 0.15, 3wAF: 0.54 ± 0.09, 6mAF: 0.55 ± 0.12, all $n = 7$, ns).

In 16/21 experiments, we compared the dissociation map with the underlying endocardial bundle structure (*Figure 5*, lower right panel). On average for all groups, EED was higher in thick areas of the atrial wall (thick: 49.3 ± 21.4%, thin: 42.2 ± 19.0%, $n = 16$, $P < 0.05$). The difference was similar in the aAF group (thick: 29.7 ± 10.8%, thin: 23.7 ± 11.1%, $n = 7$, $P < 0.01$) compared with the 6mAF group (thick: 67.8 ± 12.5%, thin: 59.0 ± 11.4%, $n = 7$, $P < 0.01$). Endo-epicardial electrode distance decreased from 3.0 ± 0.4 mm in the aAF group to 2.5 ± 0.3 mm in the 6mAF group, reflecting moderate thinning of the dilated atria during 6 months of AF ($P < 0.05$).

3.4 Incidence of breakthrough

The proportion of wave starting points located within the mapping area increased significantly from 0.8 ± 0.6/s in the aAF group to 6.2 ± 3.1/s in the 3wAF group and 13.6 ± 5.3/s in the 6mAF group ($P < 0.001$). Both epicardial and endocardial breakthroughs were included in the analysis.

3.5 Endo-epicardial dispersion of refractoriness and fractionation of atrial electrograms

All animals in persistent AF (3wAF and 6mAF group) could be successfully cardioverted by internal DC shock. No apparent differences for pacing thresholds were noticed between the endo- and epicardium. Endocardial ERPs were significantly longer when compared with the corresponding epicardial ERPs at both 250 and 400 ms in the aAF group. After 6 months of AF, there was no more statistical significant difference between the epicardial and the endocardial ERPs (*Table 2*).

Importantly, both the incidence of short double potentials and the fractionation intervals were larger after 3 weeks of AF when compared with aAF and further increased after 6 months of AF (*Figure 6* and *Table 2*). Complex-fractionated electrograms (three or more deflections) were observed only in 6mAF goats. Of note, one of the epicardial deflections coincided ($\Delta t < 2$ ms) with the endocardial deflection in 87% of all short double potentials.

3.6 Histology

In the 6mAF group, myocyte diameters were significantly larger than in the 3wAF group and the aAF group (10.9 ± 0.6 μm aAF, 13.6 ± 1.0 μm 3wAF, 17.0 ± 1.6 μm 6mAF, $P < 0.05$ 6mAF vs. 3wAF and aAF). Intermyocyte distances as a measure of extracellular matrix were larger in the 6mAF group (6.8 ± 1.6 μm) than in the 3wAF group (2.3 ± 0.3 μm, $P < 0.05$) and the aAF group (1.8 ± 0.2 μm, $P < 0.05$). No significant differences were found for these parameters between the aAF and the 3wAF group (see Supplementary material online, *Figure S3* for examples).

4. Discussion

Local heterogeneities in conduction and conduction block owing to increasing electrical uncoupling between muscle bundles have been

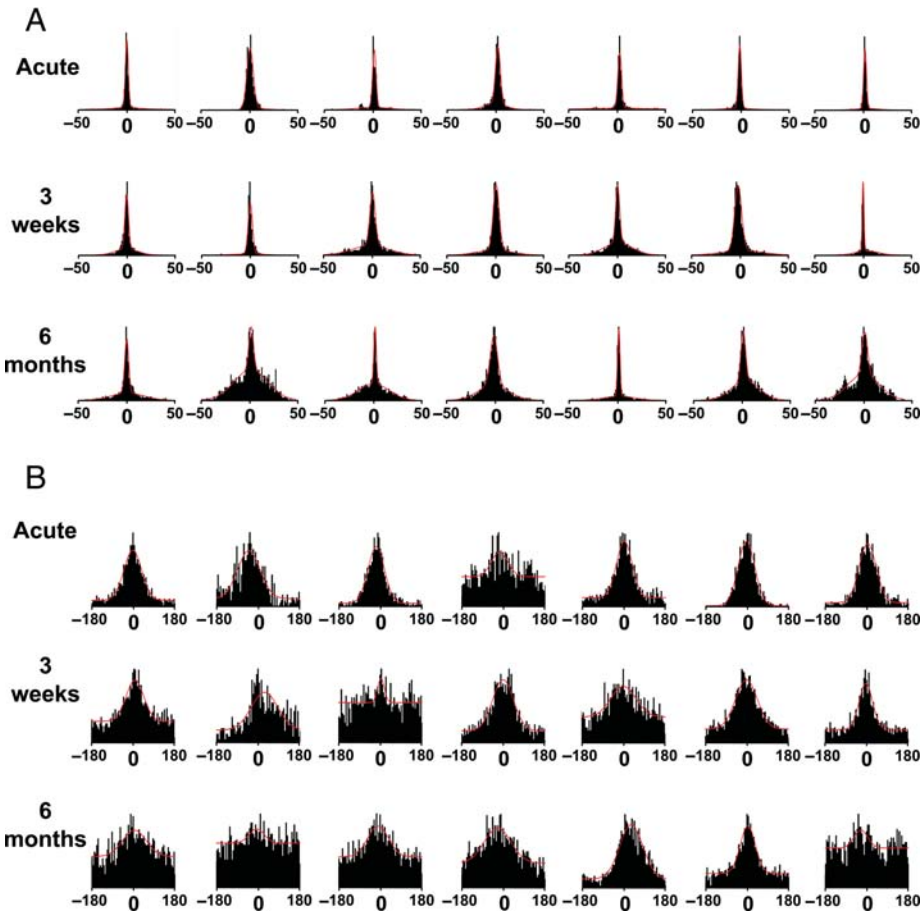

Figure 4 (*A*) Endo-epicardial activation time difference histograms of all 21 individual goats. X-axes depict activation time differences between corresponding endo-epicardial electrode pairs in milliseconds, y-axes depict number of events (normalized to allow comparison of groups). Red-fitted lines represent the curves resulting from the two-component Gaussian mixture distribution. The relative contribution of the dissociated component (low peak, wide SD) increases with AF duration (upper to lower row). (*B*) Endo-epicardial difference in directions of local conduction vector histograms of all 21 individual goats. X-axes depict difference in direction (−180 to +180 degrees); y-axes depict number of events (normalized to allow comparison of groups). Red-fitted lines represent the curves resulting from the Gaussian/uniform mixture distribution. The relative contribution of the dissociated component (uniform distribution) increases with AF duration.

suggested to contribute to increasing complexity and stability of AF over time. Dissociation of electrical activity between the epicardial layer and the endocardial bundle network has been postulated and was seen as a prerequisite for epicardial breakthrough events,[9,15,19] which more frequently occur in complex substrates for AF.[20] However, data directly addressing the existence of EED are sparse,[10,11,19] and its development during structural remodelling has not been studied so far. Our study confirms the existence of electrical dissociation between the epicardial layer and the endocardial bundle network during AF. EED was reflected both by dyssynchronous activation of the epicardial layer and the endocardial bundle network and by differences in the direction of propagation. We demonstrate that during the development of a substrate of AF, the complexity of conduction patterns is associated with a pronounced increase in EED. Importantly, this process still continues after electrical remodelling has occurred. EED is not randomly distributed but more pronounced in thicker regions of the atrial wall. The main mechanism resulting in EED during AF is not related to transmural dispersion of refractoriness but to progressive electrical uncoupling between the epicardial layer and the endocardial bundle network.

4.1 Comparison with previous studies

Schuessler *et al.*[10] were the first to directly demonstrate endo-epicardial dyssynchrony of activation during acetylcholine-induced AF in canine right atria. They demonstrated that during acute AF, endo-epicardial activation time differences became larger, particularly in thicker areas of the atrial wall and in areas with several layers with different bundle orientations. Our study extends these findings to changes occurring as a consequence of AF-induced structural remodelling and an analysis of EED based on differences in propagation direction. We confirmed that in the left atrium, EED is more pronounced in thicker parts of the atrium than in thinner parts. However, with increasing duration of AF, the thickness of the atrial wall declined while EED significantly increased. This suggests a more important role of AF-induced structural remodelling than of the absolute thickness of the atrial wall for the occurrence of EED.[14]

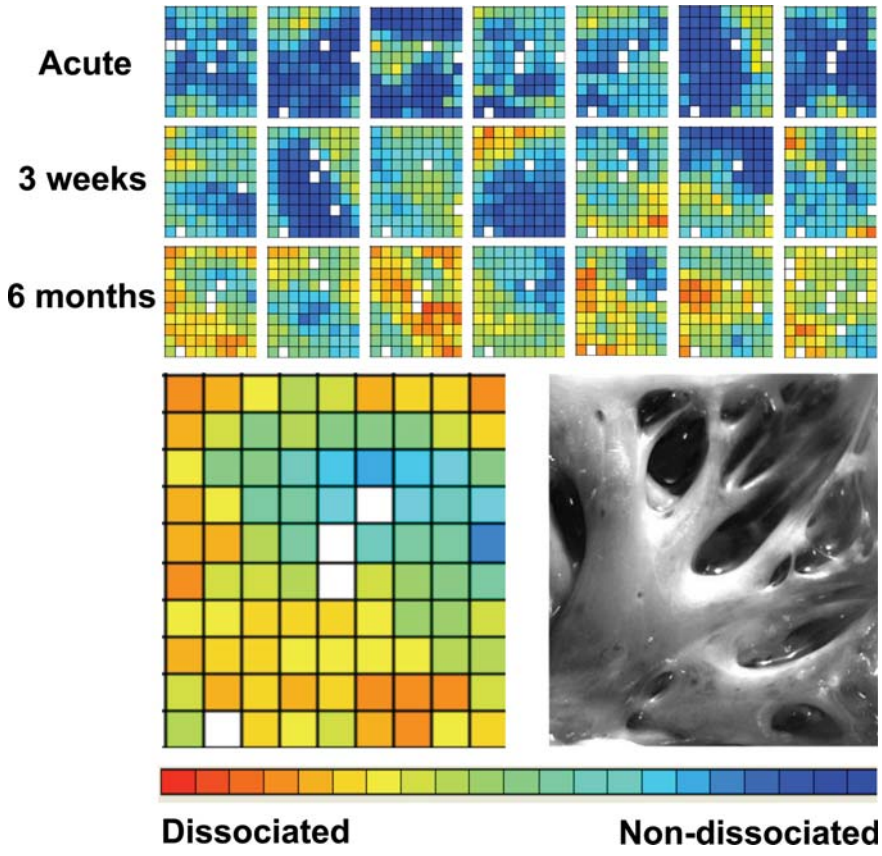

Figure 5 Upper panel: Dissociation maps of all 21 goats indicating spatial distribution of dissociation in each individual goat. Blue colour indicates little to no dissociation, red colour indicates pronounced dissociation. Colour changes toward yellow and red indicate that dissociation increases with AF duration. Inhomogeneous patterns of spatial distribution of dissociation within individual maps are apparent, indicating an influence of underlying atrial structure on the degree of dissociation. Lower left: Individual dissociation map of a goat after 6 months AF. Lower right: Corresponding endocardial bundle structure.

Table 2 Electrogram fractionation and endo-epicardial ERP differences

	Acute	3 weeks	6 months
ΔERP (endo-epicardial, ms)	21.8 ± 18	17.3 ± 8[a]	3.7 ± 16[a,b]
Fractionated electrograms (%)	9.4 ± 1.9	12.8 ± 2.7[a]	18.6 ± 0.6[a,b]
Separation interval (ms)	4.8 ± 0.5	6.1 ± 0.5[a]	9.4 ± 0.6[a,b]

Endocardial ERPs were longer when compared with epicardial only at baseline ($P < 0.001$), but not after 6 months AF. Fractionation and separation interval during rapid atrial pacing increased significantly with AF duration.
[a]Significant vs. aAF.
[b]Significant vs. 3 weeks-AF.

Epicardial mapping studies in patients with persistent AF have demonstrated that the incidence of epicardial breakthrough, i.e. transmural conduction of a wavefront from the opposing side of the atrial wall, increases with increasing duration of AF and increasing complexity of the conduction pattern.[7,20] The present study supports this finding and offers an explanation for the increased incidence of epicardial breakthroughs. It demonstrates that during the development of the substrate for AF, electrical dissociation between the endocardial bundle network and the epicardial layer progressively increases and because of this, fibrillatory conduction gradually becomes more a three-dimensional process. As EED is the prerequisite condition for breakthroughs to occur, enhanced EED might underlie the high incidence of breakthrough in a complex substrate for AF.

Recently, Everett *et al.*[11] compared virtual endocardial electrograms (Ensite®) with epicardial direct contact electrograms in four different canine models (congestive heart failure, mitral regurgitation, rapid atrial pacing, and methylcholine-induced AF). Their analysis focused on differences in electrogram morphology and revealed the largest endo- to epicardial differences in the rapid atrial pacing model. Dominant frequencies of electrical activation were lower in the endocardium than in the epicardium. However, the study by Everett *et al.* did not show whether the endo-epicardial differences in electrogram morphology, recorded with two different techniques, indeed resulted in differences in activation times and propagation direction of fibrillation wavefronts. In our study, direct contact unipolar electrograms were used for analysis of activation times on both sides of the atrial wall using a tool with precisely aligned electrode pairs. Our measurements did not show different activation rates in the endocardium vs. epicardium, but a comparable AFCL in both layers of the atrial wall. The electrophysiological changes in the rapid atrial pacing group of Everett *et al.* and the 3 weeks persistent AF group of the present study are likely to be comparable. In both

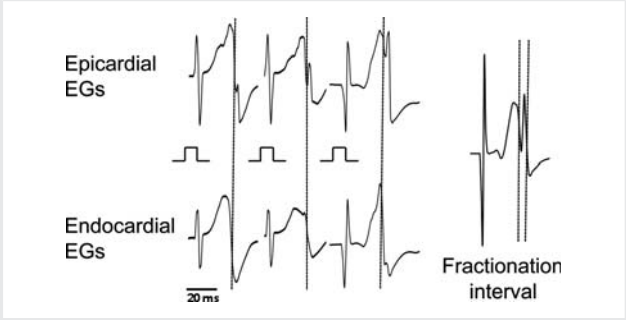

Figure 6 Left: Examples of epicardial short double potentials during rapid atrial pacing. In each example, one of the two epicardial deflections after the pacing artefact coincides with an endocardial activation and represents a farfield signal (dotted lines). Right: Time interval between first and second deflection was determined and taken as fractionation interval (between dotted lines). EGs, Electrograms.

models, significant endo-epicardial dissociation of electrical activity occurs. In models of structural remodelling of the atria, however, like for example congestive heart failure or mitral valve regurgitation, macro-reentry often underlies AF. In the study by Everett *et al*., indeed a lower incidence of conduction block and less electrical dissociation was observed in the mitral valve regurgitation model and the heart failure model compared with the RAP model. This might explain why in these models only little dissociation between the epicardial and endocardial layers was observed. In contrast, in goats with 6 months of AF, the combination of electrical remodelling and significant extracellular matrix alterations might underlie the pronounced electrical dissociation within and between the endo- and epicardial layer of the atrial wall.

4.2 Potential mechanisms leading to endo-epicardial dissociation

Structural changes in the atria and gap junction remodelling during the course of AF have been extensively studied in our model.[13,14,21–23] Van der Velden *et al*.[23] demonstrated a heterogeneous reduction in Cx40 (but not Cx43) over a time course of several months. After 9–23 weeks of AF, Ausma described that up to 92% of myocytes showed marked ultrastructural changes and a marked increase in myocyte size by 195%.[13] In this study, extracellular matrix fraction per myocyte was significantly increased both in right and in left atria after 4 months of AF. In the present study, histological analysis confirmed significant myocyte hypertrophy and—more importantly—a pronounced increase in intermyocyte distances owing to enhanced extracellular matrix formation. Spach and Dolber[6] have shown that in ageing atria, this pattern of interstitial fibrosis may lead to disruption of electrical side-to-side connections, impaired conduction, and the occurrence of fractionated electrograms. In our study, we hypothesize that electrical side-to-side connections are not only disrupted within the epicardial layer but also between the epicardial layer and the endocardial bundle network. To support this hypothesis, we demonstrated enhanced fractionation of electrograms in broad wavefronts during atrial pacing with increasing duration of AF. One of the epicardial deflections coincided with a local endocardial deflection in most cases, suggesting that fractionation was owing to a slight dyssynchrony in the activation of the epicardial layer and the endocardial bundle network. Enhanced electrogram fractionation owing to EED was associated with longer AF duration and increasing local heterogeneity, suggesting that it contributes to the complexity of the substrate and the stability of the arrhythmia.

We also addressed the question whether endo-epicardial dispersion of refractoriness might have contributed to EED during AF. Indeed, we found that at baseline, endocardial ERPs were longer than epicardial ERPs (*Table 2*). The transmural dispersion of refractoriness was smaller in the 3wAF group and after 6 months no endo-epicardial dispersion of refractoriness was detectable anymore. Wang *et al*.[24] studied endo- and epicardial action potential durations in superfused atrial tissue of guinea pigs. These authors demonstrated longer action potential durations in the endocardial than the epicardial layer presumably owing to larger transient outward currents (I_{to}) in the epicardium. Downregulation of I_{to} during AF[25] might have contributed to the reduction of transmural ERP dispersion in the atria of animals in the 3wAF and the 6mAF groups. Regardless, the underlying mechanism of the endo-epicardial dispersion of refractoriness at baseline, we conclude that endo-epicardial differences in refractoriness do not play a role in the enhancement of EED with increasing duration of AF.

4.3 Contribution of endo-epicardial dissociation to the AF substrate

EED could lead to increased AF stability by different mechanisms. First, it increases the functional area available for wavefront propagation. EED thereby enables the coexistence of more wavelets. Secondly, EED forms the prerequisite for transmural conduction. The more the epicardial layer and the endocardial bundle network are activated out of phase, the more likely a fibrillation wave will encounter excitable tissue on the other side of the atrial wall and transmurally propagate from the endocardial bundle network to the epicardial layer or vice versa. Each breakthrough might then develop into an independent fibrillation wave contributing to the fibrillation process. In this sense, breakthroughs represent additional reentry points for reactivation of areas that just regained excitability.

4.4 Potential limitations

The mapping tool was designed for endo-epicardial mapping of the left atrial free wall in a heart exposed by left-sided thoracotomy. Whether our findings are applicable for other atrial regions, with different bundle anatomy, warrants further investigation.

4.5 Conclusions

AF stability progressively increases with AF duration even after electrical remodelling has occurred. During the first 6 months, increasing AF stability is associated with an increase in EED. Not endo-epicardial dispersion of refractoriness, but progressive electrical uncoupling between the epicardial layer and the endocardial bundle network is the underlying mechanism. EED leads to AF stabilization by providing more functional surface for fibrillation wavelets to coexist and represents a prerequisite condition for transmural conduction with reactivation of atrial myocardium in the opposing layer of the atrial wall. The mechanisms described are likely to contribute to the progressive stability of AF over time by increasing the complexity of three dimensional fibrillation patterns.

Supplementary material

Supplementary material is available at *Cardiovascular Research* online.

Conflict of interest: none declared.

Funding

This work was supported by the Leducq Foundation (07 CVD 03), Dutch Heart Foundation (2005.B112), and Dutch Research Organization (NWO, VIDI-grant 016.086.379).

References

1. Kopecky SL, Gersh BJ, McGoon MD, Whisnant JP, Holmes DR Jr., Ilstrup DM *et al*. The natural history of lone atrial fibrillation. A population-based study over three decades. *N Engl J Med* 1987;**317**:669–674.
2. Zrenner B, Ndrepepa G, Karch MR, Schneider MA, Schreieck J, Schomig A *et al*. Electrophysiologic characteristics of paroxysmal and chronic atrial fibrillation in human right atrium. *J Am Coll Cardiol* 2001;**38**:1143–1149.
3. Allessie MA, Lammers W, Bonke F, Hollen J. Experimental evaluation of Moe's multiple wavelet hypothesis of atrial fibrillation. In: Zipes D, Jalife J, eds. *Cardiac Electrophysiology and Arrhythmias*. New York: Grune & Stratton; 1985. p265–275.
4. Allessie MA, Ausma J, Schotten U. Electrical, contractile and structural remodeling during atrial fibrillation. *Cardiovasc Res* 2002;**54**:230–246.
5. Wijffels MC, Kirchhof CJ, Dorland R, Allessie MA. Atrial fibrillation begets atrial fibrillation. A study in awake chronically instrumented goats. *Circulation* 1995;**92**: 1954–1968.
6. Spach MS, Dolber PC. Relating extracellular potentials and their derivatives to anisotropic propagation at a microscopic level in human cardiac muscle. Evidence for electrical uncoupling of side-to-side fiber connections with increasing age. *Circ Res* 1986; **58**:356–371.
7. Allessie MA, de Groot NM, Houben RP, Schotten U, Boersma E, Smeets JL *et al*. The electropathological substrate of longstanding persistent atrial fibrillation in patients with structural heart disease: longitudinal dissociation. *Circ Arrhythm Electrophysiol* 2010; doi:10.1161/CIRCEP.109.910125. Published online ahead of print 18 August 2010.
8. Verheule S, Tuyls E, Van Hunnik A, Kuiper M, Schotten U, Allessie MA. Fibrillatory conduction in the atrial free walls of goats in persistent and permanent atrial fibrillation. *Circ Arrhythm Electrophysiol* 2010; doi: 10.1161/CIRCEP.109.931634. Published online ahead of print 11 October 2010.
9. Konings KT, Kirchhof CJ, Smeets JR, Wellens HJ, Penn OC, Allessie MA. High-density mapping of electrically induced atrial fibrillation in humans. *Circulation* 1994;**89**: 1665–1680.
10. Schuessler RB, Kawamoto T, Hand DE, Mitsuno M, Bromberg BI, Cox JL *et al*. Simultaneous epicardial and endocardial activation sequence mapping in the isolated canine right atrium. *Circulation* 1993;**88**:250–263.
11. Everett TH, Wilson EE, Hulley GS, Olgin JE. Transmural characteristics of atrial fibrillation in canine models of structural and electrical atrial remodeling assessed by simultaneous epicardial and endocardial mapping. *Heart Rhythm* 2010;**7**:506–517.
12. de Haan S, Greiser M, Harks E, Blaauw Y, van Hunnik A, Verheule S *et al*. AVE0118, blocker of the transient outward current (I(to)) and ultrarapid delayed rectifier current (I(Kur)), fully restores atrial contractility after cardioversion of atrial fibrillation in the goat. *Circulation* 2006;**114**:1234–1242.
13. Ausma J, van der Velden HM, Lenders MH, van Ankeren EP, Jongsma HJ, Ramaekers FC *et al*. Reverse structural and gap-junctional remodeling after prolonged atrial fibrillation in the goat. *Circulation* 2003;**107**:2051–2058.
14. Ausma J, Wijffels M, Thone F, Wouters L, Allessie MA, Borgers M. Structural changes of atrial myocardium due to sustained atrial fibrillation in the goat. *Circulation* 1997;**96**: 3157–3163.
15. Holm M, Johansson R, Brandt J, Luhrs C, Olsson SB. Epicardial right atrial free wall mapping in chronic atrial fibrillation. Documentation of repetitive activation with a focal spread–a hitherto unrecognised phenomenon in man. *Eur Heart J* 1997;**18**: 290–310.
16. Kanagaratnam P, Kojodjojo P, Peters NS. Electrophysiological abnormalities occur prior to the development of clinical episodes of atrial fibrillation: observations from human epicardial mapping. *Pacing Clin Electrophysiol* 2008;**31**:443–453.
17. Gonzalez RC, Woods RE, Eddins SL. *Digital Image Processing Using MATLAB*. New Jersey: Prentice Hall; 2003.
18. Konings KT, Smeets JL, Penn OC, Wellens HJ, Allessie MA. Configuration of unipolar atrial electrograms during electrically induced atrial fibrillation in humans. *Circulation* 1997;**95**:1231–1241.
19. Eckstein J, Verheule S, de Groot N, Allessie MA, Schotten U. Mechanisms of perpetuation of atrial fibrillation in chronically dilated atria. *Prog Biophys Mol Biol* 2008;**97**: 435–451.
20. de Groot NMS. Mapping and ablation of atrial tachyarrhythmias. Thesis. Maastricht, The Netherlands: Maastricht University. 2006.
21. Ausma J, Wijffels M, van Eys G, Koide M, Ramaekers F, Allessie MA *et al*.. Dedifferentiation of atrial cardiomyocytes as a result of chronic atrial fibrillation. *Am J Pathol* 1997;**151**:985–997.
22. Neuberger HR, Schotten U, Blaauw Y, Vollmann D, Eijsbouts S, van Hunnik A *et al*.. Chronic atrial dilation, electrical remodeling, and atrial fibrillation in the goat. *J Am Coll Cardiol* 2006;**47**:644–653.
23. van der Velden HM, Ausma J, Rook MB, Hellemons AJ, van Veen TA, Allessie MA *et al*.. Gap junctional remodeling in relation to stabilization of atrial fibrillation in the goat. *Cardiovasc Res* 2000;**46**:476–486.
24. Wang ZG, Fermini B, Nattel S. Repolarization differences between guinea pig atrial endocardium and epicardium: evidence for a role of Ito. *Am J Physiol* 1991;**260**: H1501–H1506.
25. Van Wagoner DR, Pond AL, McCarthy PM, Trimmer JS, Nerbonne JM. Outward K+ current densities and Kv1.5 expression are reduced in chronic human atrial fibrillation. *Circ Res* 1997;**80**:772–781.
26. McFarlane Mood A, Graybill FA, Boes DC. *Introduction to the Theory of Statistics*. New York, NY: McGraw-Hill Companies; 1974.